Design, Synthesis, and Physicochemical and Biological Characterization of a New Iron Chelator of the Family of Hydroxychromenes

Marco Ferrali,*,† Sabrina Bambagioni,‡ Antonio Ceccanti,‡ Donato Donati,‡ Gianluca Giorgi,‡ Marco Fontani,‡ Franco Laschi,‡ Piero Zanello,‡ Mario Casolaro,§ and Antonello Pietrangelo||

Departments of Physiopathology and Experimental Medicine, Chemistry and Chemical and Biosystem Sciences and Technology, University of Siena, via Aldo Moro, I-53100 Siena, Italy, and Department of Medicine and Medical Specialities, University of Modena and Reggio Emilia, Largo del Pozzo, 71, I-41100 Modena, Italy

Received August 6, 2002

Increasing evidence suggests that iron plays an important role in tissue damage both during chronic iron overload diseases (i.e., hemochromatosis) and when, in the absence of actual tissue iron overload, iron is delocalized from specific carriers or intracellular sites (inflammation, neurodegenerative diseases, postischaemic reperfusion, xenobiotic intoxications, etc.). In the present work, we appropriately modified an iron chelator of the hydroxychromene family in order to obtain a tridentate chelator that would inactivate the iron redox cycle after its complexation, with a view to using this molecule in human therapy and/or in disease prevention. We synthesized such a chelator for the first time and show, by different physicochemical analysis, its tridentate nature and, importantly, its capacity to chelate iron with enough strength to inhibit both iron-dependent H_2O_2 generation and lipid peroxidation in in vitro biological systems.

Introduction

It is well-known that iron plays a primary role in mammalian life and in all living cells. It is usually transported and stored by specific proteins which allow the physicochemical control of the metal during and after its redox activity. If, for different reasons, iron is released from these proteins, or is excessively absorbed by liver from food, it becomes extremely dangerous for cells and the tissues by entering a redox cycle which generates toxic free radicals.[1,2] These chemically active species, which originate from the reaction of free iron with molecular oxygen or hydrogen peroxide by the Fenton and/or Haber−Weiss reactions, cause the cells to undergo lipid peroxidation,[3] protein oxidation,[4] and DNA damage.[5]

There is increasing evidence of direct or indirect involvement of iron in human diseases such as haemochromatosis,[6] thalassemias,[7] neurodegenerative diseases,[8] cancer,[9] and in all pathological states of free radical-mediated tissue damage.[10−12] Thus the goal of improving the quality of life of people affected by severe iron overload (in particular, by haemochromatosis and thalassemia) has been the stimulus to develop drugs that would increase iron excretion in man.

To this end several naturally occurring molecules and synthetic products have been tested in the past decades. Despite their disadvantages, desferrioxamine, hydroxypyridones, and pyridoxal hydrazones are the most effective chelators currently used in human therapy.[13−16]

Chart 1

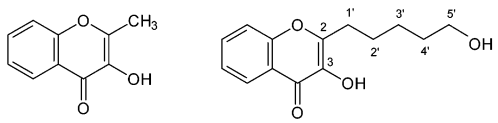

Undesirable effects of prolonged treatments with such drugs are obviously related to direct toxicity of the molecules or to iron deprivation of the bone marrow.[17,18] The ideal chelator should remove only the excess of iron from its natural carriers, but producing such a chelator is obviously extremely difficult. The picture is complicated by the fact that the chelator should not be toxic, should be suitably lipophilic to enter the cell, should chelate iron intracellularly, and should be rapidly excreted by urine and/or bile. Due to the wide variety of diseases in which iron chelators need to be utilized, it is important to continue to search for novel chelators.[19] This can be achieved either by improving known drugs or by proposing suitable new molecules in order to obtain compounds showing different affinities for iron.

In a previous paper we suggested that the 3-hydroxychromen-4-ones could be assessed as iron-chelating agents in vivo.[20] We showed that 3-hydroxy-2-methylchromen-4-one (IC_1, Chart 1) chelates iron(III) in vitro and possesses a good affinity for the metal ion. This could guarantee the lack of effect of the chelator toward iron transported by biological carriers, but it remains to be seen whether iron should be still redox active after chelation. As a bidentate ligand, IC_1 leaves two coordination sites of the Fe^{III} ion unoccupied,[20] making it likely to not be sufficiently inert for redox reactions. In fact, IC_1 is not able to inhibit iron-induced lipid peroxidation in hepatic microsomal preparations in vitro (unpublished personal observations).

With a view to developing a new synthetic iron chelator with a higher affinity for iron and keeping the

* To whom correspondence should be addressed. Phone: +39-0577-234007. Fax:+39-0577-234009. E-mail: ferrali@unisi.it.
† Department of Physiopathology and Experimental Medicine, University of Siena.
‡ Department of Chemistry, University of Siena.
§ Department of Chemical and Biosystem Sciences and Technology, University of Siena.
|| Department of Medicine and Medical Specialities, University of Modena and Reggio Emilia.

10.1021/jm021022u CCC: $22.00
Published on Web 11/15/2002

Scheme 1

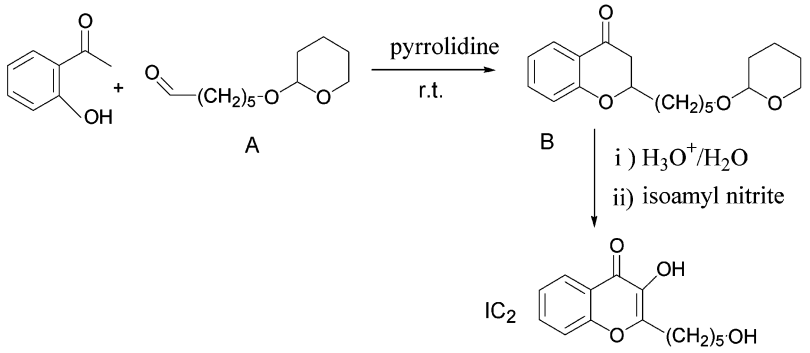

IC_1 structure as the basic molecule, we synthesized a new molecule: 3-hydroxy-2-(5-hydroxypentyl)chromen-4-one (IC_2, Chart 1). The aim was to obtain a tridentate chelator capable of enhancing the stability constant of the iron complex in order to obtain a complete inhibition of the redox cycle of iron in biological systems. We chose to use the basic IC_1 structure, rather than considering alternative molecular structures due to the fact that the chromanic ring is common to tocopherols and this results in good lipophilicity and low toxicity for most synthetic derivatives. The characterization of the molecule and preliminary in vitro and in vivo studies on its possible use in the biological environment are presented in this paper.

Results and Discussion

The synthesis of the 3-hydroxy-2-(5-hydroxypentyl)-chromen-4-one (IC_2) was accomplished as described in Scheme 1.

The synthesis of IC_2 starts from the monolateral protection of an alcoholic group of 1,6-hexanediol by reaction with 2,4-dihydropyran. This procedure allows the next monolateral oxidation of the 6-(tetrahydropyran-2-yloxy)hexan-1-ol to 6-(tetrahydropyran-2-yloxy)-hexanal (Scheme 1, A) with pyridinium chlorochromate (see Experimental Section for further details). The carbonyl group is the means by which the condensation of the last product with 2′-hydroxyacetophenone takes place in the presence of pyrrolidine. The subsequent cyclization in the pyranic ring, after water is lost, is immediate and spontaneous giving 2-[5-(tetrahydropyran-2-yloxy)pentyl]chroman-4-one (Scheme 1, B). The hydroxylation of the latter compound is obtained by the reaction with isoamyl nitrite after removal of the pyrane protection to avoid possible interference of the pyrane displaced during the reaction, yielding IC_2. The combined analyses of the purified product obtained, by ^1H NMR, ^{13}C NMR in $CDCl_3$, mass spectrometry, and X-ray diffraction (Figure 1) assured the identity of the final product (see Experimental Section). The IC_2 is a colorless solid with a melting point of 112−114 °C; it is a fluorescent product having an ex_{max} at 335 nm and an em_{max} at 485 nm in CH_2Cl_2 solution. Its mass spectrum shows the molecular ion at *m*/*z* 248 (rel inten 15%) and two very abundant ions at *m*/*z* 189 (75%) and 176 (100%) both corresponding to the fragmentation of the aliphatic side chain.

The X-ray structure of IC_2 is illustrated in Figure 1. The heterocyclic system is planar with the largest deviation (0.047(4) Å) shown by C(4) from its least-squares plane. The distance O(2)···O(3), which constitutes the two most probable sites for iron chelation, is equal to 2.767(4) Å, which is very close to the value of 2.734(3) Å found in IC_1.[20] In the crystal lattice, O(2)−H participates in intra- and intermolecular hydrogen bonding with O(3) and stacking interactions occur between the heterocyclic systems.

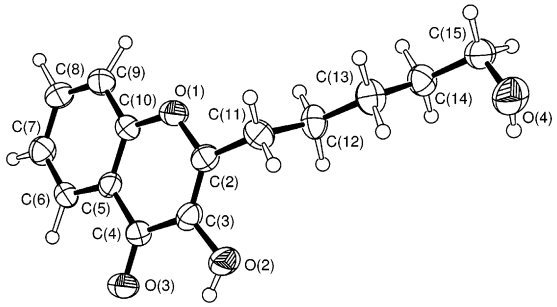

Figure 1. X-ray crystal structure of 3-hydroxy-2-(5-hydroxypentyl)chromen-4-one (IC_2).

Spectrophotometric analysis of the dynamics of the complex formation with iron(III) shows that 2 mol of the chelator are engaged in the complexation of 1 mol of iron (Figure 2). The isosbestic point of the spectra at 335.5 nm is evident until the concentration of the iron rises from zero to half the concentration of the chelator (Figure 2A−D). When the iron concentration exceeds this value (Figure 2E), spectral changes are evident, reasonably due to the presence of an excess of uncomplexed $FeCl_3$. In fact a solution of 100 μM $FeCl_3$ in the same buffer shows an absorbance of 0.180 and 0.250 au at 335.5 and 300 nm, respectively (not shown).

Mass Spectrometry of the Complex. Different mass spectrometry ionization techniques, i.e., LSIMS and ESI, were used for the structural characterization of the complex obtained by mixing $FeCl_3$ and IC_2 in methanol. Both LSIMS and ESI show the presence of intense ions at *m*/*z* 550 corresponding to an Fe(III):IC_2 ratio of 1:2, while species with different molar ratios were not detectable.

The product ion spectra, ranging from MS^2 to MS^4, obtained by ESI of the iron complex, are reported in Figure 3. The main decompositions obtained by selecting the ions at *m*/*z* 550 as the main beam (Figure 3A) consist in the loss of one and two water molecules yielding ions at *m*/*z* 532 and 514, respectively. The MS^3 spectrum of ions at *m*/*z* 532 (Figure 3B) shows the loss of 54 mass units corresponding to C_4H_6 from the side chain producing the species at *m*/*z* 478. Also ions at *m*/*z* 514 eliminate 54 mass units yielding ions at *m*/*z* 460 (Figure 3C).

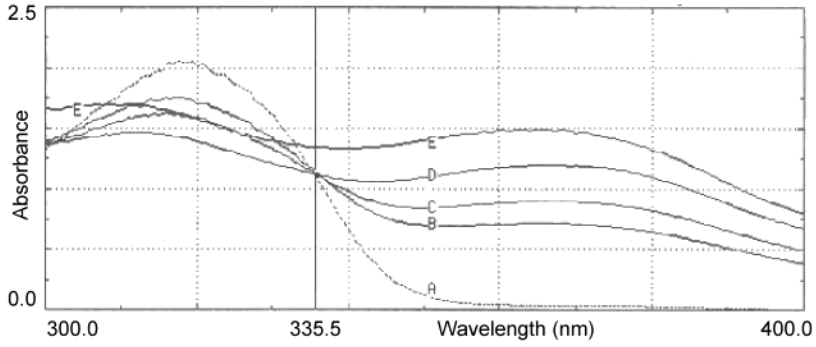

Figure 2. Spectrophotometric detection of Fe(III) complexation with IC_2: (A) spectrum of 200 μM IC_2 in Tris-Maleate buffer pH 7.4; (B−E) spectra of IC_2 after the addition of 50, 70, 100, and 200 μM $FeCl_3$, respectively. See Experimental Section for details.

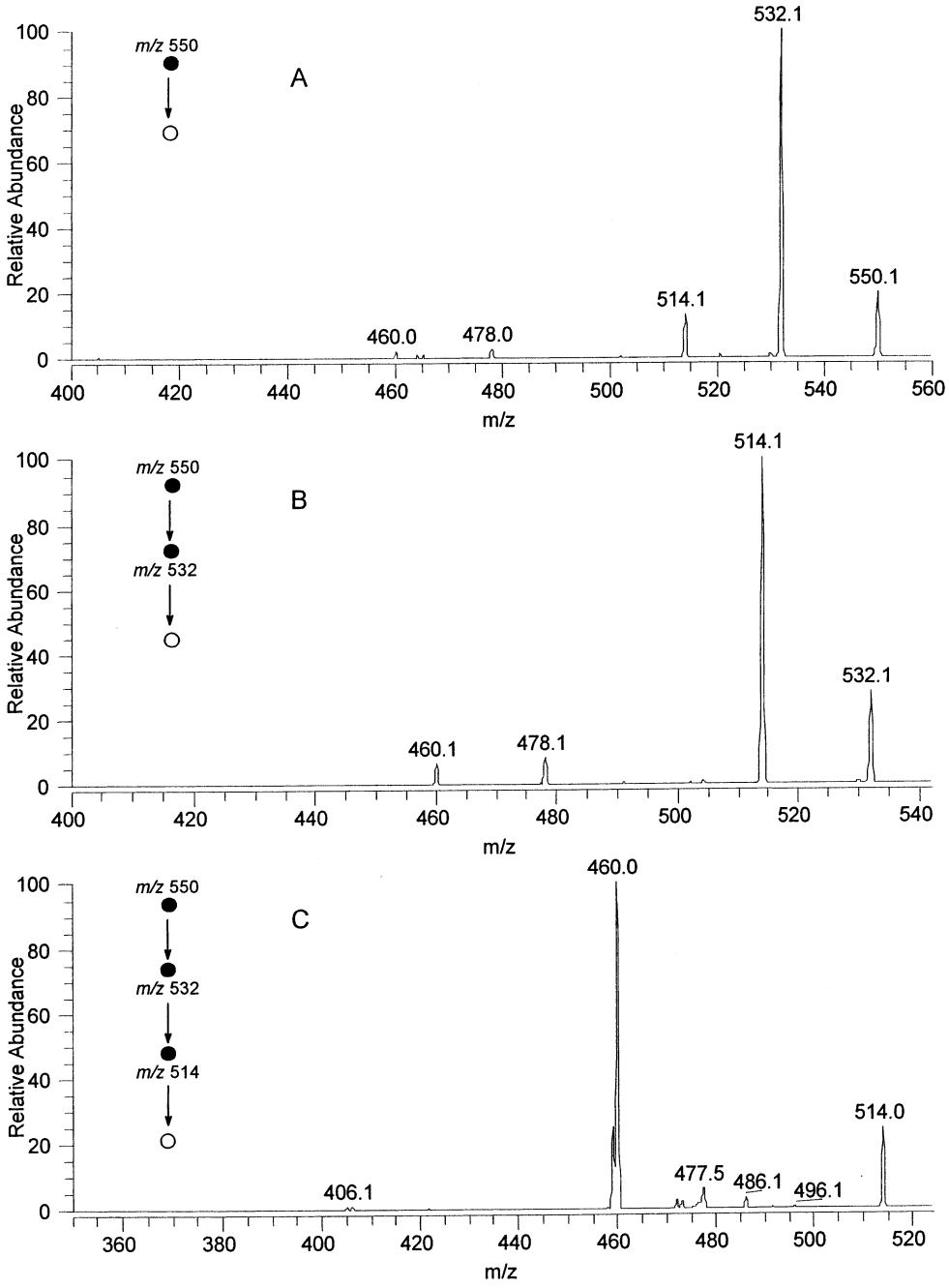

Figure 3. Electrospray MS^n experiments of the [Fe^{III}−((IC_2)$_2$ − 3H)] complex in methanol. (a) MS/MS of the species at *m*/*z* 550; (b) MS^3 of the cations at *m*/*z* 532; (c) MS^4 of the species at *m*/*z* 514.

After having unambiguously determined that the species formed by mixing $FeCl_3$ and IC_2 is detected at *m*/*z* 550, we have to establish whether this species is a charged ion already present in solution or whether it is produced by a protonation reaction due to ionization. The study of negative ions was able to clarify this point. When we used LSIMS in negative mode we obtained very intense ions at *m*/*z* 549, while under ESI (−) conditions a species is detected at *m*/*z* 548, with very scarce abundance. This apparent disagreement can be rationalized by considering that under LSIMS (−) conditions a radical anion can be formed. On the other hand, this process is highly unfavored under the ESI (−) regime where radical ions are only seldom observed. The prevailing process under ESI (−) conditions is the abstraction of a proton that for this complex is very unfavored, as shown by the scarce abundance of ions at *m*/*z* 548. It follows that the species detected at *m*/*z* 550 both under LSIMS and ESI is formed by protonation during the ionization, and it is reasonably attributed to $[Fe(IC_2 - H)(IC_2 - 2H) + H]^+$. On the other hand, the negative ions at *m*/*z* 549 (LSIMS) and *m*/*z* 548 (ESI) are due to $[Fe(IC_2 - H)(IC_2 - 2H)]^{-\bullet}$ and $[Fe(IC_2 - H)(IC_2 - 2H) - H]^-$, respectively.

This suggests that by mixing $FeCl_3$ and IC_2 a neutral complex with stoichiometry $[Fe(IC_2 - H)(IC_2 - 2H)]$ is obtained. It implies a deprotonation of one ligand on the oxygen at position 3 of the pyran ring, while the other ligand undergoes a double deprotonation of both the hydroxy groups. This suggests that the oxygen of the long side chain participates in the chelation of the iron(III) ion.

Mass spectrometry experiments aimed at evaluating the chelating strength of IC_2 toward Fe(III) were also carried out. By mixing a solution of the complex $[Fe^{III}(IC_1 - H)_2]^+$ with IC_2, in a 1:1 molar ratio, the coordination strength of IC_2 causes the removal of the iron from the complex with $IC_1$and ions at *m*/*z* 550 are produced in very high abundance. This suggests that IC_2 has much stronger coordinating properties than IC_1 toward Fe(III) ions.

Potentiometry. Potentiometric measurements in aqueous solution have been performed to further study the formation of the iron(III) complex with IC_2. The free ligand IC_2 is scarcely soluble in water at low pH, but its solubility increases sharply above pH 7. The original colorless solution becomes yellow in the alkaline region because of the ionization of the OH group(s) that may trigger electron delocalization along the carbon rings. Protonation of the ionized groups was easily recognized from the buffered region appearing in the potentiometric curve. The computed basicity constant value ($\log K = 8.88 \pm 0.04$) is close to that of the homologous ligand IC_1 (8.90 ± 0.03), thus suggesting that ionization of the ligand really involves the OH group directly linked to the ring.

Unlike protonation, the complex formation equilibrium occurs only in the low pH region. The dark-violet solution of the iron(III) complex becomes clearer as the ligand improves its solubility in the presence of Fe(III) ions. As the pH reaches the alkaline region, the iron complex is destroyed and the solution again assumes the yellow color of the free ligand. The best potentiometric curve is obtained with a ligand/metal molar ratio close to 2.5. Only in this case the stoichiometry of the complex species of $Fe^{III}(IC_2)_2H_{-3}$ fits the potentiometric curve and an estimated stability constant log β is obtained. The log β value of −1.76 for the reaction: $Fe(III) + 2IC_2 = Fe^{III}(IC_2)_2H_{-3} + 3H^+$ suggests deprotonation of the coordinating ligand. In particular, three protons for each Fe(III) ion are titrated before the sharp equivalent point. The splitting-off of three protons in the acidic region is compatible with the very high stability constant value (log $\beta' = 26$) of the direct reaction: $Fe(III) + IC_2H_{-2} + IC_2H_{-1} = Fe^{III}(IC_2)_2H_{-3}$. It is noteworthy that the iron(III) complex forms even in the low pH region.

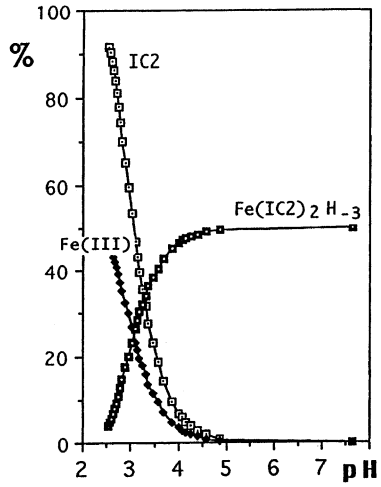

Figure 4. Computed species distribution plot of the ligand IC_2 and Fe(III) system. (IC_2/Fe molar ratio of 2:1; $[IC_2] = 0.4$ mM, $[Fe^{III}] = 0.2$ mM).

Figure 4 shows a plot of the species distribution curves obtained by taking into account only the complex formation equilibrium at the ligand/metal molar ratio of 2:1. It is evident that complexation reaches its maximum at pH 5, when the concentration of the free Fe(III) ion is close to zero. Extrapolation to the latter concentration at pH 7.4 gives a pFe(III) = 16.3. This value is obtained when the calculation is made with total concentrations of ligand and Fe(III) ion of 10^{-5} and 10^{-6} M, respectively.[15] The calculated pFe(III) value can be considered on the borderline where the hydrolysis reaction of the metal may occur. In our case this reaction occurs only in alkaline conditions and above the physiological pH.

From the potentiometric data we can reasonably hypothesize that the Fe(III) ion coordinates with the tridentate ligand according to an octahedral geometry giving rise to a neutral complex.

X-Band EPR Analysis. Figure 5 compares the X-band EPR spectra of the $Fe^{III}(IC_2)_2$ complex recorded in CH_2Cl_2 solution (Figure 5A,B) with that of $Fe^{III}Cl_3$ (Figure 5C). The line shape analysis confirms the metal-centered nature of the paramagnetic signal ($g_i \neq g_{electron} = 2.0023$) for the two iron complexes, and the pertinent parameters are consistent with a $S = 5/2$, Fe(III) high spin state (Table 1). Such features can be accounted for the strong magnetic effect of the Zero Field Splitting interaction, typical of $S > 1/2$ system.[21,22]

Because of the strong interplay between the ligand framework and the $S = 5/2$ electrons of the Fe(III) ion, such an interaction affords significant variations in the

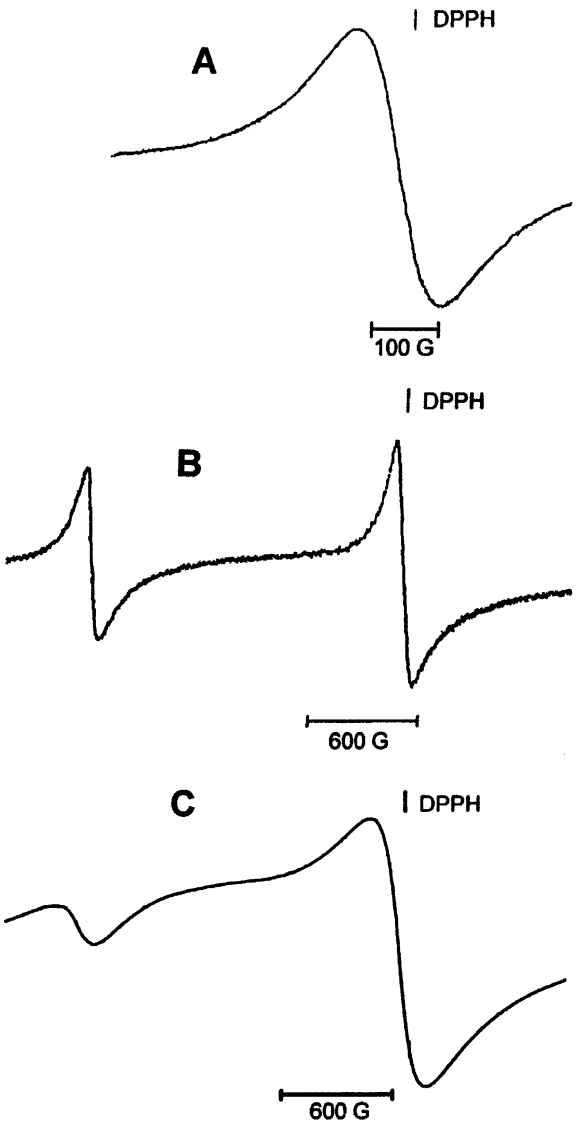

Figure 5. X-Band EPR spectra of the [Fe^{III}−((IC_2)$_2$ − 3H)] complex in CH_2Cl_2 at room temperature (298 K) (A), 100 K (B), and $FeCl_3$ at 100 K (C).

Table 1. X-band EPR Parameters of the Fe^{III}−L and Fe^{III}−Cl_3 Complexes in CH_2Cl_2 Solution[a]

complex	g_{iso}	g_{aniso}	ΔH_{iso}	ΔH_{aniso}
Fe^{III}−IC_2	2.017(6)	2.012(8)	135(8)	70(8)
		4.257(8)		100(8)
Fe^{III}−IC_1	2.014(5)	2.016(6)	130(6)	120(6)
		4.259(6)		130(6)
Fe^{III}−Cl_3	2.027(8)	2.014(8)	290(30)	220(30)
		3.738(8)		340(30)

[a] g_{iso}, ΔH_{iso}: T = 298 K; g_{aniso}, ΔH_{aniso}: T = 100 K; ΔH values in Gauss.

line shape and important dependence of the paramagnetic parameters upon different experimental conditions. Accordingly, the signals are broad and unresolved (Figure 5).[23,24] No metal hyperfine or ligand superhyperfine interactions (if any) are present either in glassy or fluid solutions (^{57}Fe: natural abundance = 2.15%, I-^{57}Fe = 1/2).

Table 1 points out the significant effect played by IC_1 and IC_2 ligands on the S = 5/2 Electron Spin Fe^{III} system in comparison with $Fe^{III}Cl_3$: a noticeable difference in both ΔH_i and g_i values occurs. Moreover, the

Chart 2

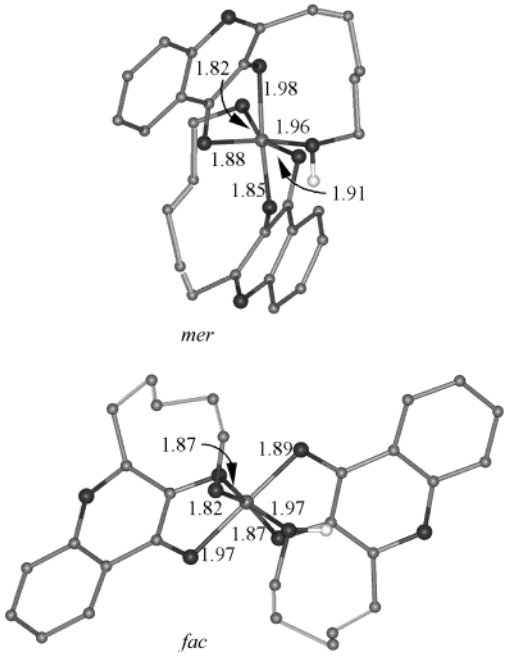

increase in ΔH_{aniso} values of $Fe^{III}(IC_1)_2$ with respect to $Fe^{III}(IC_2)_2$ likely reflects differences in apical coordination (z axis). The bidentate IC_1 ligand leaves the axial position open to different coordinating species, whereas the tridentate IC_2 ligand occupies all the coordination sites, thus causing significant geometrical constraints (see the geometry optimization section).

In fluid solution, the intense adsorption of $Fe^{III}(IC_2)_2$ becomes quite symmetrical (g_{iso} = 2.017(6)) (first and second derivative spectra) and unresolved, due to the overall isotropic line width, ΔH_{iso} = 135(8) G, which largely overlaps the underlying S = 5/2 fine structure.

Geometry Optimization of $Fe^{III}(IC_2)_2$ Complex. On the light of satisfactory performances in geometry optimization of transition metal complexes,[25] we adopted PM3 semiempirical method to optimize the molecular structure of $Fe^{III}(IC_2)_2$ in the gas phase. The complex assumes an highly distorted octahedral coordination. The *mer*-isomer results only 17 kJ/mol more stable than the *fac*-isomer (see Chart 2).

Electrochemistry. Since electrochemical investigations are commonly employed to determine the coordinating ability of siderophores,[20,26−29] a cyclic voltammetric study was performed in order to compare the affinity of the IC_2 ligand for Fe(III) ion with those of the IC_1 precursor and of the well-known desferrioxamine B (DEF) (Figure 6A).

Given that, in agreement with the above-mentioned potentiometric and mass spectrometric measurements, preliminary voltammetric experiments on each ligand confirm that both IC_1 and IC_2 form stable complexes with Fe(III) ion in a ligand-to-metal ratio of 2:1, whereas DEF forms the 1:1 complex, it is immediately evident that, as expected,[20] the original Fe(III)/Fe(II) reduction of $FeCl_3$ (E_{pc} = +0.29V, vs SCE) upon complexation undergoes cathodic shifts which are a function of the nature of the different ligands. In addition, the quasi-reversible character of the one-electron reduction of $FeCl_3$ (ΔE_p = 410 mV at 0.05 Vs^{-1}) becomes irreversible upon complexation (see below).

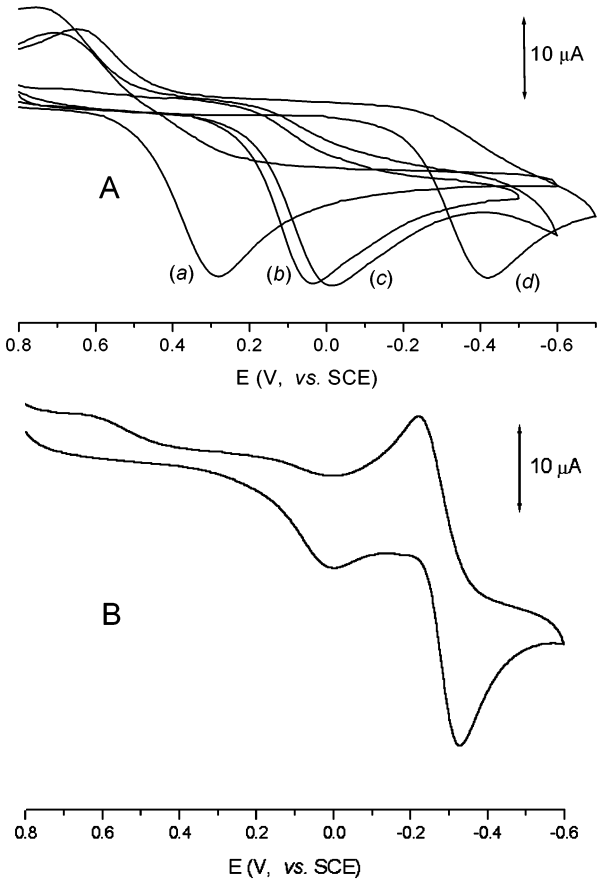

Figure 6. (A) Cyclic voltammetric profiles recorded at a glassy carbon electrode on methanol solutions containing $[NBu_4]ClO_4$ (0.1 M) and (a) $FeCl_3$ (1.6 mM), (b) $FeCl_3$ (1.6 mM) + IC_1 (4.8 mM), (c) $FeCl_3$ (1.8 mM) + IC_2 (5.4 mM); (d) $FeCl_3$ (1.7 mM) + DEF (3.4 mM). (B) Cyclic voltammogram recorded at a platinum electrode on a methanol solution containing $[NBu_4]ClO_4$ (0.1 M) and $FeCl_3$ (1.8 mM) + IC_2 (5.4 mM). Scan rate 0.05 V s^{-1}.

From a qualitative viewpoint, Figure 6A immediately proves that the coordinating ability of IC_2 ligand toward Fe(III) ion is somewhat higher than that of IC_1 (E_{pc} = −0.01V (IC_2) and + 0.05V (IC_1) vs SCE), but notably lower than that of DEF (E_{pc} = −0.42V, vs SCE). This was further supported by competition experiments. As a matter of fact, both the addition of IC_2 ligand to solution of $Fe(IC_1)_2$, and addition of DEF ligand to $Fe(IC_2)_2$ ultimately leads to the voltammetric profiles of $Fe(IC_2)_2$ and Fe(DEF), respectively.

The shift of the redox potential of free metal ions upon complexation is strictly related to the stability constant values of the involved redox couples according to the relationship:[30]

$$(E^{\circ\prime})_{complex} = (E^{\circ\prime})_{free} - 0.059 \log \frac{\beta_{ox.}}{\beta_{red.}}$$

which holds in those cases in which the complex formed by each member of the redox couple involves the same number of ligand molecules. In these cases the electrode potential of the redox processes does not vary with the ligand concentration. Assuming that the electrode potential of free Fe(III)/Fe(II) ion in aqueous solution ($E^{\circ\prime}$ = +0.51 V, vs SCE) [31] also holds in methanol solution, the data summarized in Table 2 are obtained.

Table 2. Stability Constant Values of Fe(III) Complexes Derived from Electrochemical Data.

ligand	$\log \beta_{Fe(III)}/\beta_{Fe(II)}$	$\log \beta_{Fe(III)}$	$\log \beta_{Fe(II)}$
IC_1	8.0	–	–
IC_2	8.8	≥26[a]	19.2
DEF	15.8	31[a,b]	15.2

[a] From potentiometric data in acid solution; [b] From ref 32.

Since $\log \beta_{Fe(III)}$ values have been obtained in acid solutions, it is evident that the $\log \beta_{Fe(II)}$ values calculated here are purely speculative. For example, a $\log \beta_{Fe(II)}$ value of 10.0 has been calculated from the electrochemical investigation of Fe(III)(DEF) in strong alkaline solution (pH 10.5).[28]

In support of the deprotonation reaction observed both by potentiometric or mass spectrometric methods upon mixing $FeCl_3$ and IC_2, Figure 6B shows the cyclic voltammogram obtained at a platinum electrode in a methanol solution of $FeCl_3$ in the presence of IC_2 (in 1:3 ratio). As seen, the previously discussed irreversible $Fe^{III}(IC_2)_2$ reduction (E_p = −0.01 V) is followed by a major (about three time more intense) reversible reduction ($E^{\circ\prime}$ = −0.27 V). Such a reduction process was coincident with the proton reduction experimentally observed on a methanol solution containing 3 mM HCl. Under the same experimental conditions the use of a glassy carbon electrode makes the proton reduction irreversible and shifts toward much more negative potential values (E_p = −1.0 V), thus explaining the clear picture illustrated in Figure 6A.

Finally, we point out that the irreversibility of the Fe(III)/Fe(II) reduction upon complexation suggests that in all cases the instantaneously electrogenerated Fe(II) complex monoanion is not stable under the original ligand composition which stabilizes the Fe(III) ion.

Iron-Dependent H_2O_2 and TBARS Formation. The central focus of our work is to build a chelator able to inhibit iron-dependent biological oxidative stress, that is, to make iron electrochemically inert in the biological environment after its complexation. Therefore we performed a series of experiments to evaluate this important aspect. We previously realized that the bidentate chelator IC_1 was not able to inactivate the iron-redox cycle and thus prevent oxidative stress in in vitro biological systems (Ferrali, unpublished results). The higher affinity of the new chelator for Fe(III), as deduced from electrochemistry, potentiometry, and mass spectrometric measurements, suggests that IC_2 could prevent the redox activity of the Fe(III) ion. To verify this hypothesis, rat liver microsomes were incubated in vitro in an iron-dependent pro-oxidant system and, separately, hydrogen peroxide production and lipid peroxidation evolution were evaluated. It is well-known that, in the presence of dioxygen, iron ions easily generate hydrogen peroxide which, in turn, catalyzes the hydroxyl radical formation widely assumed to be responsible for oxidative alteration of membrane phospholipids.[2] The biological membranes we prepared allowed us to obtain microsomes with sufficient lysosome contamination, to have a moderate initiation and propagation of the iron-dependent lipid peroxidation without addition of NADPH or other reducing agents.[33]

Figure 7 shows the results obtained for H_2O_2 formation. As can be observed, the production of H_2O_2 strongly increases when iron−ADP complex is added as an

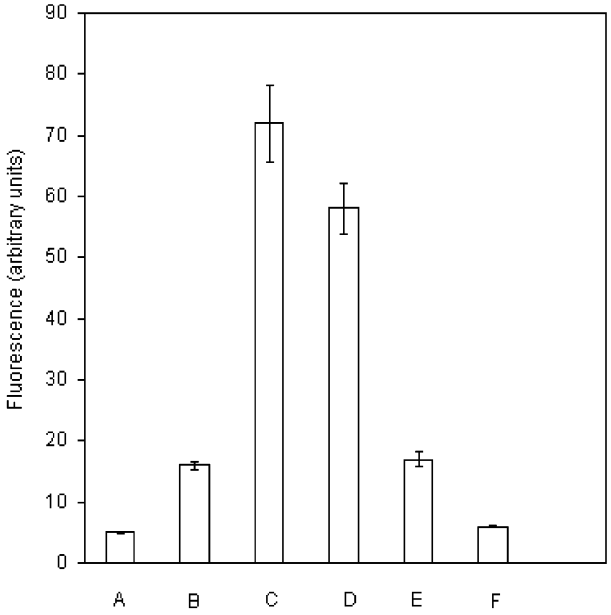

Figure 7. Iron-dependent H_2O_2 formation in rat liver microsomal preparations (MC). A: Control MC with the only addition of 2.5 mM ADP; B: MC as in A plus DCFA; C: complete system (plus 100 μM $FeCl_3$); D: as in C plus 100 μM IC_2; E: as in C plus 200 μM IC_2; F: control MC plus 2.5 mM ADP plus15 μM IC_2 plus DCFA. (for further details see Experimental Section). The final microsomal protein concentration was about 0.08 mg/mL. Values represent the mean of three separate experiments ± SE.

oxidant trigger (Figure 7C) to control microsomes (Figure 7B). The concomitant presence of the chelator at a concentration double that of Fe(III) ion completely prevents its oxidative effect (Figure 7E). On the other hand, when the concentration of the chelator is the same as that of the metal, leaving 50 μM iron free, no significant inhibition is observed (Figure 7D). This suggests that the new chelator, IC_2, is able to inactivate the iron redox cycle only when all the metal is sequestered, excluding an aspecific antioxidant activity of the molecule. The H_2O_2 production in this case is almost the same of that produced by 100 μM iron because, at these concentrations (that is 30−100 μM), the relationships between dose−effect is not linear. Also worthy of attention is the finding that the addition of 15 μM IC_2 to the control microsomes (Figure 7F) completely abolishes the spontaneous production of H_2O_2, the residual fluorescence being due to ADP per se (Figure 7A). This suggests that redox active iron contamination in liver microsomal preparations is no more than 6−7 μM. Measurements of H_2O_2 production have also been performed in the presence of 0.2 mM NADPH as biological reducing agent. In the presence of ADP−iron, DCFA oxidation, in this case, is about double when compared to that obtained without reductant. Nevertheless, the presence of 200 μM IC_2 completely inhibits again H_2O_2 formation (data not shown).

In another series of experiments using higher concentration of microsomes, we measured thiobarbituric acid-reactive substance (TBARS) formation as an index of lipid peroxidation, which should approximately be proportional to H_2O_2 formation.

As can be seen in Figure 8, while the control rat liver microsomes do not produce any significant TBARS formation (Figure 8A), the addition of 100 μM iron by

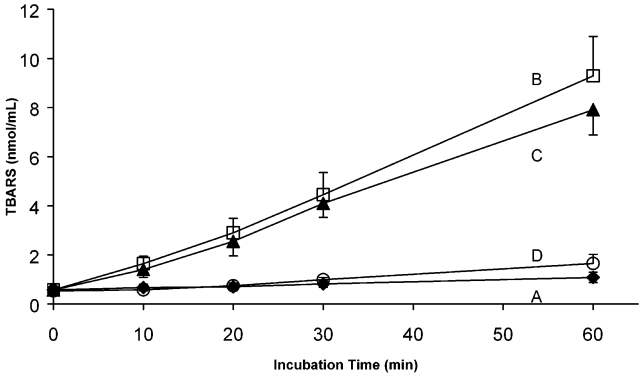

Figure 8. Iron-dependent TBARS evolution in rat liver microsomal preparations (MC). A: Control MC; B: MC plus 100 μM $FeCl_3$, 2.5 mM ADP; C: as in B plus 100 μM IC_2; D: as in B plus 200 μM IC_2. The microsomal protein concentration was 1.5 mg/mL. Values represent the mean of four separate experiments ± SE.

means of the ADP−Fe complex causes the appearance of TBARS in the incubation medium at a concentration of about 10 μM (Figure 8B) whereas the presence of 200 μM IC_2 completely prevents TBARS formation (Figure 8D). Again, as with H_2O_2 formation, 100 μM of the chelator practically does not affect the extent of lipid peroxidation (Figure 8C). Similarly to H_2O_2 formation, TBARS evolution has been evaluated also in the presence of 0.2 mM NADPH as reductant. In this case ADP−iron complex causes a TBARS concentration increase at 40 μM after 60 min of incubation being about 30 μM just after 10 min. Nevertheless, as seen with H_2O_2 formation, the presence of 200 μM IC_2 completely prevents TBARS development (about 1.5 μM after 60 min; not shown). Therefore on the basis of these biological experiments, we can conclude that the new chelator, IC_2, maintains the iron in a sufficiently stable complex to prevent its redox cycle in biological systems.

Conclusions

We previously suggested that, when suitably modified to chelate iron, the chromanic ring, which characterizes the polar head of vitamin E, could be useful as iron sequestering agent both in vitro and in vivo. The first molecule that we proposed (IC_1) binds iron but does not inhibit the iron redox cycle in vitro so that it is difficult to think that it could be suitable for iron chelation therapy. Therefore we undertook to modify IC_1 so as to increase its affinity for iron sufficiently to prevent its redox cycle after its complexation. Our novelty is to substitute the methyl group in IC_1 with an aliphatic alcoholic chain long enough to carry the terminal alcoholic oxygen in the core of the iron coordination site of the expected complex. The designed molecule is unknown, and its synthesis has been reported for the first time and described in detail in the present work. The synthetic procedure appears to be suitable to provide a few grams of the final product at a time. A series of chemicophysical investigations, such as spectrophotometry, mass spectrometry, potentiometry, EPR, and electrochemistry demonstrated that IC_2 binds Fe(III) in a 2:1 molar ratio. IC_2 acts as a tridentate and, importantly, the affinity for iron ($\log \beta \geq 26$) is high enough to inhibit the iron redox cycle in the biological environment despite the fact that it is lower than that

of desferrioxamine and hydroxypyridones (log $\beta = 31$ and log $\beta = 36$, respectively). The electrochemical study of the complexation between $FeCl_3$ and IC_2 shows that the reduction potential of its complex is higher than that of IC_1 but lower than that of ferrioxamine, thus confirming that desferrioxamine has higher affinity than IC_2 for iron. In our opinion, this finding is very important in view of the possible use of the new chelator as an in vivo sequestering agent; it is possible, in fact, that the undesirable side effects of the chelators already in use are due to their excessive affinity for body iron.

It is really important that once iron is chelated it must be not able to enter the redox cycle. The experiments carried out on iron-dependent hydrogen peroxide formation and TBARS evolution clearly demonstrate that when iron is chelated by IC_2 it is not redox active in biological systems such as hepatic microsomal suspensions not even in the presence of biological reductans. This means that, at least in the liver, an environment suitable to reach the reduction potential of the IC_2-complexed iron does not exist.

IC_2 is a lipophilic compound and, like IC_1,[20] crosses erythrocyte membranes, is absorbed in rodents after both intraperitoneal and intragastric administration, and is excreted within 24−48 h via the urine (unpublished personal observations).

These observations strongly suggest that our expectation of improving the iron affinity of the chromanic ring in IC_1 by adding the aliphatic alcoholic chain in the 2 position of the IC_1 has been completely vindicated. The new molecule acts as a tridentate chelator and, importantly, inhibits the iron redox cycle after its chelation in the in vitro biological systems. Therefore it is reasonable to continue to study this compound especially in view to demonstrate its ability to remove, in a redox inactive form, the excess of body iron in the cases of iron overload.

Experimental Section

1,6-Hexanediol was from Fluka, 2′-hydroxyacetophenone, 3,4-dihydro-2*H*-pyran, pyridinium chlorochromate, pyrrolidine, and isoamyl nitrite were supplied by Aldrich, and ADP and dichlorofluorescein were from Sigma. Others salts and solvents were of analytical grade. The NMR analyses were performed using a Bruker AC 200 MHz instrument; melting points were detected by a Mettler TA instrument DSC 12 E. Elementary analysis was evaluated by a 240 Perkin-Elmer analyzer. Gas chromatography−mass spectrometry (GC-MS) experiments were carried out by a Varian Saturn 2000 ion trap instrument coupled with a gas chromatograph Varian Star 3400 CX equipped with a column J&W DB5-MS (30m × 0.25 mm, film thickness 0.25 μm) by using ultrapure helium as a carrier gas. Fluorimetric analysis were performed by a 650−10S Perkin-Elmer fluorimeter.

6-(Tetrahydropyran-2-yloxy)hexan-1-ol. A 100 g (0.5 mol) amount of 1,6-hexanediol are dissolved in 38 mL (0.5 mol) of 2,4-dihydropyran and maintained at room temperature in a water bath After adding about 50 mg of *p*-toluensulfonic acid, the mixture is allowed to react for about 2 h under magnetic stirring. An aqueous solution of K_2CO_3 is then added, and the reaction products are extracted with diethyl ether. Three different compounds are detected by GC-MS, and these are the unreacted 1,6-hexanediol, 1,6-dioxopyranylhexane, and about 70% of 6-(tetrahydropyran-2-yloxy)hexan-1-ol.

6-(Tetrahydropyran-2-yloxy)hexanal. According to the work of Kasmai et al.,[34] a solution of 15 g of pyridinium chlorochromate in 400 mL of dichloromethane is added to 20 g of the crude mixture from the former reaction, and the mixture is stirred at room temperature. After 90 min, the solvent is evaporated and the residual slurry is washed several times with a petroleum ether/ethyl ether (1:1) solution. The yield of this oxidation step was about 60%, as estimated by GC-MS.

2-(5-Hydroxypentyl)chroman-4-one. According to the work of Kabbe and Widdig,[35] about 15 g of crude products from the former reaction are placed in a two-neck round-bottom flask and 2.1 g (30 mmol) of pyrrolidine are added, drop by drop, under magnetic stirring, keeping the solution at room temperature by a water bath. A 4.1 g (30 mmol) amount of 2′-hydroxyacetophenone were then added and the formation of the condensation product was monitored by TLC (silica gel, with petroleum ether/ethyl ether 3:1 as eluent). After about 90 min, the pyrrolidine is removed by vacuum evaporation, and water is added to the mixture and extracted by ethyl ether. After evaporation, an oily residue containing the 2-[5-(tetrahydropyran-2-yloxy)pentyl]chroman-4-one is obtained.

To remove the protecting pyranyl group, the residue is dissolved in about 20 mL of ethanol with the addition of concentrated HCl (25 mL). The formation of a compound with lower R_f was monitored by TLC using ethyl acetate/petroleum ether (30:70) as the eluent. After about 60 min at room temperature, the ethanol is evaporated. The aqueous mixture is neutralized with a K_2CO_3 solution and then extracted with ethyl ether. After evaporation of the organic phase, the residue was chromatographed using a silica column with ethyl acetate/petroleum ether (70:30) as the eluent, obtaining the final product 2-(5-hydroxypentyl)chroman-4-one. Yield: 50%. ^{1}H NMR ($CDCl_3$): δ 6.95−7.85 (m, 4H, aromatic), 4.45 (tdd,1H, $J = 7.9$, $J = 8.20$, $J = 6.25$ Hz, H(2)), 3.67 (t, 2H, $J = 7.4$ Hz, H(5′)), 2.69 (dd, 2H, $J = 6.25$, $J = 8.20$ Hz, H(3)), 1.4, 1.9 (m, 8H, H(1′), H(2′), H(3′), H(4′)).

3-Hydroxy-2-(5-hydroxypentyl)chromen-4-one (IC_2). Following the procedure of Geissman and Armen,[36] 10 mmol (2.3 g) of 2-(5-hydroxypentyl)chroman-4-one is dissolved in 70 mL of 90% ethanol at 45−50 °C, and 30 mmol of isoamyl nitrite and 100 mmol of concentrated HCl are added, drop by drop contemporaneously. The reaction is carried out until the starting compound disappears in TLC (about 90 min). Then the reaction mixture is neutralized with K_2CO_3-saturated water solution and extracted with ethyl acetate. The oily residue is fractionated using silica gel column chromatography and eluting with ethyl acetate/petroleum ether (70:30). After evaporation of the solvent a yellow solid is recovered. Several crystallizations from acetone at first and then from ethyl ether allowed us to obtain a gas chromatographically pure, colorless, solid of IC_2. Yield about 50%. Anal. ($C_{14}H_{16}O_4$) C, calcd 67.74, found 67.78; H, calcd 6.45, found 6.74. Mp 112−114 °C; ^{1}H NMR ($CDCl_3$): δ 7−3−8.3 (m, 4H, aromatic), 3.68 (t, 2H, $J =$ 6.3 Hz, H(5′)), 2.88 (t, 2H, $J = 7.4$ Hz, H(1′)), 1.5, 1.9 (m, 6H, H(2′), H(3′), H(4′)); ^{13}C NMR ($CDCl_3$): δ 25.36, 26.43, 28.83, 35.35, 62.66, 118.07, 121.50, 124,28, 125.46, 132.95, 138.25, 152.34, 155.57, 172.250; *m*/*z* (EI) 248 (M^+, 15), 189 (75), 176 (100); HRMS Calcd for $C_{14}H_{16}O_4$ *m*/*z* 248.1049, found: *m*/*z* 248.1049.

X-ray Crystallography. Single crystals of IC_2 were obtained by dissolving a few milligrams of IC_2 in acetone and allowing the solution to concentrate at room temperature. A colorless single crystal of approximate dimensions 0.15 × 0.35 × 0.15 mm was submitted to X-ray analysis using a Siemens P4 four-circle diffractometer with graphite monochromated Mo−Kα radiation ($\lambda = 0.71069$ Å). Lattice parameters were determined by least-squares refinement on 46 randomly selected and automatically centered reflections. The $\omega/2\Theta$ scan technique was used and the data were collected in the $2 \leq \Theta \leq$ 26° scan range. Crystal system: monoclinic; space group: $P2_1/c$ (no. 14); $a = 12.335(2)$, $b = 5.4090(10)$, $c = 18.721(2)$ Å, $\beta =$ 95.97(1)°, $V = 1242.3(3)$ Å^3, $Z = 4$, $D_c = 1.327$ g/cm^3. 3400 reflections were collected at 22 °C of which 2445 are unique ($R_{int} = 0.06$). Absorption correction by using the Ψ method was applied. The structure was solved by direct methods implemented in the SHELXS-97 program.[38] The refinement was carried out by full−matrix anisotropic least−squares on F^2 for

all reflections for non-H atoms by using the SHELXL-97 program.[39] The final refinement converged to $R_1 = 0.068$, $wR_2 = 0.115$ for $I > 2\sigma I$, goodness-of-fit = 0.982. Min. max height in last $\Delta\rho$ map of −0.184 and 0.195 eÅ^{-3}. Full crystallographic details will be given elsewhere.

Mass Spectrometry of the IC_2−Fe $^{3+}$ Complex. Mass spectrometry (MS) and MS/MS analyses were performed with a VG 70-250S instrument (Micromass, Manchester) using electron ionization (EI) and liquid secondary ion mass spectrometry (LSIMS) techniques; electrospray (ESI) measurements were carried out on a LCQ DECA mass spectrometer (ThermoFinnigan). One drop of a solution, obtained by dissolving a few micrograms of IC_2 and ferric chloride in methanol, was put on the stainless steel tip of the LSIMS probe, mixed with glycerol as a matrix, and exposed to the Cs^+ beam for the desorption. In ESI experiments, methanol solutions in the micromolar range were injected by direct infusion at 5 μL min^{-1}. The spray voltage and the temperature were +4.5 kV and 180 °C, respectively.

Spectrophotometric Measurements. Fresh stock solutions of 10 mM IC_2 in ethanol and 2 mM anhydrous ferric chloride in water were made. The spectrum of 200 μM IC_2 in Tris-maleate buffer pH 7.4 was detected between 300 and 400 nm. Then increasing amounts of $FeCl_3$ (50, 70, 100, and 200 μM, respectively) were added and each new spectrum detected by a DU 640 Beckman spectrophotometer.

Potentiometric Measurements. Titrations were performed at a constant temperature (25 °C) with a digital PHM-84 Radiometer potentiometer, equipped with a pHG211 High pH glass electrode and a ref 201 reference electrode (Radiometer). A Metrohm Multidosimat piston buret connected to a computer (Olivetti M20) controlled and automatically recorded potentiometric data (emf reading, mV, in relation to volume, mL, of added titrant).[39] A 0.1169 mmol amount of IC_2 was dissolved in 95 mL of 0.1 M NaCl, and 3 mL of 0.1 M NaOH was added to help its dissolution under magnetic stirring. Titration with 0.1 M HCl was performed under a presaturated nitrogen stream flowing over the surface of the solution to avoid contamination with CO_2 from the outside atmosphere. At the end of the titration, a measured quantity (0.0460 mmol) of $FeCl_3$ was added to the solution in order to have a molar ratio IC_2/Fe(III) of 2.5. The obtained dark-violet solution was titrated with a standardized NaOH solution (0.1078 M). Potentiometric data were processed with the Superquad program[40] to calculate the basicity and stability constants.

EPR Spectra. X-band EPR spectra were recorded on the BRUKER 200D-SRC spectrometer operating at 9.44 GHz. The microwave frequency was tested with a XL Microwave Frequency Counter 3120 and the external magnetic field H calibrated by using a DPPH powder sample ($g_{DPPH} = 2.0036$). The spectrometer was equipped with a low temperature device (Bruker ER 401 VT). The solid-state and solution samples were placed into calibrated quartz capillaries permanently positioned in the EPR resonance cavity. The X-band EPR averaged parameters were evaluated on the background line of the first derivative line shape of the different experimental spectra recorded at different temperatures (298 and 100 K) for both the solid-state and solution samples.

Geometry Optimization of $Fe^{III}(IC_2)_2$ Complex. PM3 semiempirical method,[41] as implemented in Hyperchem,[42] has been used to optimize the structure of the $Fe^{III}(IC_2)_2$ complex. The staring geometry of the ligand was that obtained by the X-ray study. The structure was fully optimized without any symmetry constraint. The complex has an high spin state, therefore the unrestricted formalism has been adopted for a system with $S = 5/2$. Calculations have been performed for both the *fac*- and *mer*-isomers.

Voltammetry. Materials and apparatus for cyclic voltammetry have been described elsewhere.[20] Potential values were referenced to the saturated calomel electrode (SCE). Under the present experimental conditions the one-electron oxidation of ferrocene occurs at $E^{0'} = +0.34$V, vs SCE.

Inhibition of Iron-Dependent H_2O_2 Formation in Microsomal Suspension. A 4 g amount of rat liver was homogenized in 40 mL of 50 mM Tris-maleate buffer pH 7.4 (TM) containing 150 mM KCl and 100 μM EDTA to prevent spontaneous oxidations. The homogenate was centrifuged at 10000 rpm for 20 min. The supernatant was collected and centrifuged at 80000 × g for 40 min.

The microsomal sediment was resuspended in 36 mL of 50 mM TM. This suspension was further diluted in TM buffer at the concentration of microsomes equivalent to 100 mg of liver (about 0.25 mg of protein) per 10 mL. Solutions of 5 mM ADP and 5 mM ADP plus 200 μM ferric chloride, respectively, were prepared in the same buffer. Two separate solutions of 20 mM IC_2 and 40 mM dichloro fluorescein diacetate[43] (DCFA) in ethanol were prepared. H_2O_2 formation was detected for 5 min in a fluorimeter cuvette containing 0.5 mL of microsomal suspension in buffer, 1 mL of Fe−ADP solution, and 5 μL of DCFA, to which different additions of IC_2 were made. Control measurements adding 1 mL of 5 mM ADP alone instead of ADP−Fe were also performed.

Inhibition of Iron-Dependent Microsomal Lipid Peroxidation. MC were prepared as described above and resuspended in TM buffer at the concentration of MC equivalent to 4 g of liver in 36 mL. The suspension was then adjusted, after protein measurements, at 3 mg of protein per mL. Solutions of iron-ADP and IC_2 were prepared as above. Amounts of 0.6 and 1.2 μmol of IC_2 were pipetted into separate flasks. The solvent was dried and the residue dissolved in 3 mL of the MC suspension with vigorous shaking, after which 3 mL of the iron−ADP solution was added. Control microsomes were incubated adding 3 mL of buffer instead of ADP−Fe solution. All the flasks were incubated for 60 min at 37 °C. At the indicated times, aliquots were withdrawn to measure TBARS formed.[44]

Supporting Information Available: Crystal data, atomic coordinates, anisotropic dispacement parameters, bond lengths and angles (Tables 1S−4S) of IC_2. This material is available free of charge via the Internet at http://pubs.acs.org.

Acknowledgment. We thank MURST, Rome, Italy and Consorzio Interuniversitario di Ricerca in Chimica dei Metalli nei Sistemi Biologici for financial support.

References

(1) Halliwell, B.; Gutteridge, J. M. C. Oxygen Free Radicals and Iron in Relation to Biology and Medicine: Some Problems and Concepts. *Arch. Biochem. Biophys.* **1986**, *246*, 501−514.
(2) Ryan, T. P.; Aust, S. D. The Role of Iron in Oxygen-Mediated Toxicities. *Crit. Rev. Toxicol.* **1992**, *22*, 119−141.
(3) Minotti, G.; Aust, S. D. Redox Cycling of Iron and Lipid Peroxidation. *Lipids* **1992**, *27*, 219−226.
(4) Dean, R. T.; Fu, S.; Stocker, R.; Davies, M. J. Biochemistry and Pathology of Radical-mediated Protein Oxidation. *Biochem. J.* **1997**, *324*, 1−18.
(5) Linn, S. DNA Damage by Iron and Hydrogen Peroxide *in vitro* and *in vivo*. *Drug Metab. Rev.* **1998**, *30*, 313−326.
(6) Pietrangelo, A. Metals, Oxidative Stress, and Hepatic Fibrogenesis. *Semin. Liver Dis.* **1996**, *16*, 13−30.
(7) Hershko, C.; Graham, G.; Bates, G. W.; Rachmilewitz, E. A. Non-Specific Serum Iron in Thalassemia: An Abnormal Serum Fraction of Potential Toxicity. *Brit. J. Haematol.* **1978**, *40*, 255−263.
(8) Dexter, D. T.; Jenner, P. Alterations in Iron in Neurodegenerative Disorders: Implications and Possible Therapeutic Agents. In *Mineral and Metal Neurotoxicology*; Yasui, M. et al., Eds.; CRC Press: Boca Raton, 1997; pp 365−378.
(9) Weinberg, E. D. Development of Clinical Methods of Iron Deprivation for Suppression of Neoplastic and Infectious Diseases. *Cancer Invest.* **1999**, *17*, 507−513.
(10) Galey, J. B. Potential Use of Iron Chelators Against Oxidative Damage. *Adv. Pharmacol.* **1997**, *38*, 1167−203.
(11) Ferrali, M.; Signorini, C.; Sugherini, L.; Pompella, A.; Lodovici, M.; Caciotti, B.; Ciccoli, L.; Comporti, M. Release of Free, Redox-Active Iron in the Liver and DNA Oxidative Damage Following Phenylhydrazine Intoxication. *Biochem. Pharmacol.* **1997**, *53*, 1743−1751.
(12) de Valk, B.; Marx, J. J. M. Iron, Atherosclerosis, and Ischemic Heart Disease. *Arch. Int. Med.* **1999**, *26*, 1542−1548.
(13) Giardina, P. J.; Grady, R. W. Chelation Therapy in β-Thalassemia: The Benefits and Limitations of Desferrioxamine. *Semin. Hematol.* **1995**, *32*, 304−312.

(14) Olivieri, N. F.; Brittenham, G. M. Iron-Chelating Therapy and the Treatment of Thalassemia. *Blood* **1997**, *89*, 739−761.
(15) Tilbrook, G. S.; Hider, R. C. Iron Chelators for Clinical Use. In *Metal Ions in Biological Systems;* Sigel, A.;. Sigel, H., Eds.; Marcel Dekker: New York, 1998; Vol. 35, pp 691−730.
(16) Richardson, D. R.; Ponka, P. Pyridoxal Isonicotinoyl Hydrazone and its Analogues: Potential Orally Effective Iron-Chelating Agents for the Treatment of Iron Overload Disease. *J. Lab. Clin. Med.* **1998**, *131*, 306−315.
(17) Diav-Citrin, O.; Koren, G. Oral Iron Chelation with Deferiprone. *Pediatr. Clin. North Am.* **1997**, *44*, 235−247.
(18) Cregg, L.; Hebbel, R. P.; Miller, W.; Solovey, A.; Selby, S.; Enright, H. The Iron Chelator L1 Potentiates Oxidative DNA Damage in Iron-Loaded Liver Cells. *Blood* **1998**, *32*, 632−638.
(19) Hoffbrand, A. V. Iron Chelation Therapy: The Need for Orally Active Drugs. *J. Lab. Clin. Med.* **1998**, *131*, 290−291.
(20) Ferrali, M.; Donati, D.; Bambagioni, S.; Fontani, M.; Giorgi, G.; Pietrangelo, A. 3-Hydroxy-(4H)-benzopyran-4-ones as Potential Iron Chelating Agents In Vivo. *Bioorg. Med. Chem.* **2001**, *9*, 3041−3047.
(21) Abragam, A.; Bleaney, D. *Electron Paramagnetic Resonance of Transition Ions*; Dover Publ.: New York, 1970.
(22) Mabbs, F. E.; Collison, D. *Electron Paramagnetic Resonance of d Transition Metal Compounds*, Elsevier Publ.: New York, 1992; Vol. 16.
(23) Drago, S. Electron Paramagnetic Resonance Spectra of Transition Metal ion Complexes. *Physical Methods for Chemists*; Saunders College Publishing: New York, 1992; pp 559−603.
(24) Field, D.; George, A. V.; Laschi, F.; Malouf, Y.; Zanello P. Electrochemistry of Acetylide Complexes of Iron. *J. Org. Chem.* **1992**, *435*, 347−56.
(25) Cundari, T. R.; Deng, J. PM3 Analysis of Transition-Metal Complexes. *J. Chem. Inf. Comput. Sci.* **1999**, *39*, 376−381.
(26) Harris, W. R.; Carrano, C. J.; Cooper, S. R.; Sofen, S. R.; Avdeef, A. E.; McArdle, J. V.; Raymond, K. N. Coordination Chemistry of Microbial Iron Transport Compounds. 19. Stability Constants and Electrochemical Behaviour of Enterobactin and Model Complexes. *J. Am. Chem. Soc.* **1979**, *101*, 6097−6104.
(27) Nesset, M. J. M.; Shokhirev, N. V.; Enemark, P. D.; Jacobson, S. E.; Walker, F. A. Models of the Cytochromes. Redox Properties and Thermodynamic Stabilities of Complexes of Hindered Iron(III) and Iron(II) Tetraphenylporphyrinates with Substituted Pyridines and Imidazoles. *Inorg. Chem.* **1996**, *35*, 5188−5200.
(28) Spasojeviæ, I.; Armstrong, S. K.; Brickman, T. J.; Crumbliss, A. L. Electrochemical Behaviour of the Fe(III) Complexes of Cyclic Hydroxamate Siderophores Alcaligin and Desferrioxamine E. *Inorg. Chem.* **1999**, *38*, 449−454.
(29) Serratrice, G.; Galey, J.-B.; Aman, E. S.; Dumats, J. Iron(III) Complexation by New Aminocarboxylate Chelators. Thermodynamic and Kinetic Studies. *Eur. J. Inorg. Chem.* **2001**, 471−479.
(30) Heyrovsky, I.; Kuta, J. Reversible Processes Controlled by Diffusion of Complex Ions. *Principles of Polarography*; Academic Press: New York, 1966; pp 147−160.
(31) Kolthoff, I. M.; Lingane J. J. Iron, Cobalt, Nichel and Platinum Metals. *Polarography*; Interscience Publishers: New York, 1952; pp 475−492.
(32) Evers, A.; Hancock, R. D.; Martell, A. E.; Motekaitis, R. J. Metal Ion Recognition in Ligands with Negatively Charged Oxygen Donor Groups. Complexation of Fe(III), Ga(III), In(III), Al(III), and Other Highly Charged Metal Ions. *Inorg. Chem.* **1989**, *28*, 2189−2195.
(33) Fong, K. L.; McCay, P. B.; Poyer, J. L. Evidence that Peroxidation of Lysosomal Membranes is Initiated by Hydroxyl Free Radicals Produced during Flavin Enzyme Activity. *J. Biol. Chem.* **1973**, *248*, 7792−7797.
(34) Kasmai, H. S.; Mischke, S. G.; Blake, T. J. 18-Crown-6 Complexes of *n*-Butylammonium and Pyridinium Chlorochromates. Mild and Selective Oxidizing Agents for Alcohols. *J. Org. Chem.* **1995**, *60*, 2267−2270.
(35) Kabbe, H. J.; Widdig, A. Synthesis and Reactions of 4-Chromanones. *Angew. Chem., Int. Ed. Engl.* **1982**, *21*, 247−256.
(36) Geissman, T. A.; Armen, A. The Rearrangement of 2-Acethyl- and 2-Benzoylcoumarone Oxime *p*-Toluenesulfonates. *J. Am. Chem. Soc.* **1955**, *77*, 1623−1627.
(37) Sheldrick, G. M. *SHELXS-97*, Rel. 97−2, University of Göttingen, 1997.
(38) Sheldrick, G. M. *SHELXL-97*, Rel. 97−2, University of Göttingen, 1997.
(39) Casolaro, M.; Bignotti, F.; Ferruti, P. Amphoteric Poly(amidoamine) Polymers Containing the Ethylendiamine-N,N′-Diacetic Acid Moiety. Stability of Copper(II) and Calcium(II) Chelates. *J. Chem. Soc., Faraday Trans.* **1997**, 3663−3668.
(40) Gans, P.; Sabatini, A.; Vacca, A. Superquad: An Improved General Program for Computation of Formation Constants from Potentiometric Data. *J. Chem. Soc., Dalton Trans.* **1985**, 1195−1200.
(41) Stewart, J. J. P. Optimisation of parameters for semiempirical methods. I. Method. *J. Comput. Chem.* **1989**, *10*, 209−220.
(42) Hyperchem 7.0, Hypercube Inc., Gainesville, FL.
(43) Keston, A. S.; Brandt, R. The Fluorimetric Analysis of Ultramicro Quantities of Hydrogen Peroxide. *Anal. Biochem.* **1965**, *11*, 1−5.
(44) Comporti, M.; Hartman, A.; Di Luzio, N. R. Effects of *in vivo* and *in vitro* Ethanol Administration on Liver Lipid Peroxidation. *Lab. Invest.* **1967**, *16*, 616−624.

JM021022U